PAPER • OPEN ACCESS

Optimizing ion implantation to create shallow NV centre ensembles in high-quality CVD diamond

View the article online for updates and enhancements.

Materials for **Quantum Technology**

Optimizing ion implantation to create shallow NV centre ensembles in high-quality CVD diamond

Midrel Wilfried Ngandeu Ngambou[1],*[iD], Pauline Perrin[2], Ionut Balasa[2][iD],
Ovidiu Brinza[1], Audrey Valentin[1], Vianney Mille[1], Fabien Bénédic[1][iD],
Philippe Goldner[2][iD], Alexandre Tallaire[1,2] and Jocelyn Achard[1],*[iD]

1   LSPM, CNRS, Université Sorbonne Paris Nord, 99 Avenue JB Clément 93460, Villetaneuse, France
2   Chimie ParisTech, PSL Research University, CNRS, Institut de Recherche de Chimie Paris, 75005 Paris, France
*   Authors to whom any correspondence should be addressed.

E-mail: midrel.ngandeu@lspm.cnrs.fr and jocelyn.achard@lspm.cnrs.fr

Abstract

The negatively charged nitrogen-vacancy centre (so-called NV-centre) in diamond is one of the most promising systems for applications in quantum technologies because of the possibility to optically manipulate and read out the spin state of this defect, even at room temperature. Nevertheless, obtaining high NV densities (>500 ppb) close to the surface (5–20 nm) while maintaining good spin properties remain challenging. In this work we rely on a versatile ion implantation system allowing both implanting nitrogen using N_2^+ and creating vacancies with He^+ ion bombardment at variable energies and fluence to create shallow NV ensembles. By optimizing the ion irradiation conditions as well as the surface preparation prior to treatment we successfully increase the amount of created colour centres while demonstrating narrow magnetic resonance linewidths.

1. Introduction

The nitrogen-vacancy (NV) centre in diamond is a widely studied defect that possesses unique spin and optical properties. It is indeed possible to optically initialize and readout the electronic spin state with long coherence times up to several milliseconds even at room temperature as demonstrated in [1]. These specific spin properties have paved the way to ultra-sensitive, high-performance and innovative quantum sensors (magnetometers, gyroscopes, spectrum analysers, etc) which could open up perspectives in investigating properties that remain inaccessible by conventional devices. Several proposals for integrating NV centres in sensing and quantum applications rely on their tailored fabrication in ultra-pure host material and have been used for sensing magnetic fields, spin-based qubits for quantum information processing [2–4]. To develop such devices, the diamond films must possess very high crystalline quality and the density, environment, orientation of the introduced colour centres have to be perfectly controlled. Microwave plasma-assisted chemical vapour deposition (MPACVD) has been identified as a key technology to produce such engineered 'quantum grade' diamond films [5]. Nevertheless, some of these applications require a spatial accuracy of a nanometre for positioning NV centres close to the diamond surface, which can hardly be achieved by direct CVD growth. Another important challenge is to create a high density of shallow NV centres that preserve long NV spin coherence times [6]. Several methods have been studied to overcome this difficulty such as tapered nanopillars fabrication, delta doping or diamond with an integrated RF micro-antenna for the soin manipulation of NV centre [7–9]. A well-established method to generate these centres consists in nitrogen ion implantation of a high purity CVD film followed by thermal annealing [10]. This technique has been the subject of several studies [11, 12] and a better understanding of the accumulation and generation of defects during ion implantation has been established [13].

In this paper, we report an efficient process for creating shallow NV centres in diamond using an implantation system based on the use of a single cavity electron cyclotron resonance (ECR) source module for producing relatively high energy ion beams (5–50 keV) using different gas sources. By combining nitrogen and helium ion

implantation, NV centre ensembles have been produced at a depth of 30 nm. Their creation has been optimized by choosing appropriate energies and fluence and their spin properties have been assessed by optically detected magnetic resonance (ODMR). In addition, we explored different surface treatments of the diamond prior to implantation such as surface terminations, polishing and subsequent reactive ion etching with inductively coupled plasma (RIE-ICP) etching.

2. Experimental details

A schematic diagram of our experimental system is shown in figure 1(a). It consists of a secondary vacuum system, a gas inlet, an implantation chamber and a Faraday cup, the latter allowing measuring ion current and thus assessing fluence. Ion beam is generated in the chamber using an ECR plasma system. The gas flow injected into the ECR source is controlled with a throttle valve and a pressure of about 10^{-5} mbar is maintained. The ion fluence is adjusted by setting the microwave power of the ECR source between 0.3 and 4 W. We aim at fluence below 2×10^{13} ions cm^{-2}, to avoid diamond graphitization reached at 10^{22} vac cm^{-3} [14, 15]. By applying an acceleration voltage, the ion energy can be set from 5 to 50 keV while the beam focus can be adjusted with another electrode that has to be biased to roughly 90% or less of the accelerating voltage. The beam size in this experiment is about 0.8 cm^2, i.e. larger than the size of the single crystal diamonds that are used.

Prior to implantation, 20 μm-thick high purity CVD diamond layers have been grown on type Ib high pressure high temperature (100)-oriented diamond substrates by MPACVD [16]. Following growth, the surface of the samples has been conditioned following two different treatments: (i) a hydrogen plasma performed in the CVD chamber to allow for H-termination or (ii) an ozone treatment using a deep-UV light to achieve O-termination except for sample 5 that was submitted to a low-power microwave plasma oxygen treatment (see table 1). To further assess the effect of surface states on ion implantation, another set of diamond films have been polished using a standard 'Scaife' system to a roughness of the order of $Ra = 0.1$ μm over a surface of 100×100 μm^2 as measured by optical profilometry. It has been followed by a tri-acid cleaning of H_2SO_4:$HClO_4$:HNO_3 (2:3:3). On one sample, an RIE-ICP etching with a gas mixture of Ar:O$_2$ (1:1) at a temperature of 20 °C and a pressure of 4 mbar has been performed during 7 min in order to remove around 2 μm of material off the surface. The objective of this treatment is to estimate both the impact of polishing on NV centres formation and the possibility to limit this impact by removing the hardened zone created by polishing before implantation. After polishing or ion etching, all samples were hydrogen terminated and implanted. Table 1 summarizes the surface treatments carried out on the CVD diamond layers before and after implantation. After implantation all samples were oxygen terminated in order to stabilize the shallow NV centres.

The samples have then been exposed successively to nitrogen and helium ion beams in our implantation system. The low energy of the ECR microwave source does not allow for a complete dissociation of the stable N$_2$ molecules and therefore mostly N$_2^+$ ions are created in the plasma and accelerated. These ions have been used to introduce nitrogen inside the diamond, but they also generate vacancies. The second ion beam treatment with He$^+$ ions only produces vacancies and has been used to optimize substitutional nitrogen (N$_S$) to NV conversion. Based on SRIM simulations [17], the penetration depth of those ions has been plotted in figure 1(b) as a function of acceleration voltage. In order to implant N and He at a similar depth of 30 nm, we have selected a voltage of 40 keV for N$_2^+$ (i.e. 20 keV for individual N atoms) and 5 keV for He$^+$ ions respectively.

The effect of helium has been investigated on sample No. 5 starting from hydrogen terminated ultrapure CVD diamond film firstly implanted using nitrogen ions for 10 s over the entire surface. Then, helium has been implanted in three different areas of the same sample during respectively 10, 20 and 30 s. To screen untreated areas from the beam, we used a physical shadow mask placed onto the sample. The implantation conditions are given in table 1 and a scheme of the implantation distribution for this sample is shown in figure 2.

Finally, the samples have been annealed under high vacuum (10^{-6} mbar) at 800 °C for 2 h in order to repair the damage induced by implantation and allow vacancies migrating to pair with nitrogen [17]. Figure 3 summarises the experimental process used to create NV centres.

Raman and photoluminescence (PL) measurements under optical excitation at 473 nm and 532 nm have been performed in a non-confocal mode using a Horiba-HR800 spectrometer. A DiamondViewTM instrument has been used to observe the fluorescence and phosphorescence. Confocal laser scanning microscope has been used to perform images. ODMR measurements have been performed by a confocal microscopy set-up in order to access the spin properties and measure coherence times of different implanted samples. A high numerical aperture objective (NA = 0.95) has been used to focus the excitation green laser (532 nm) on the sample and collect the PL from the NV$^-$ centres. The PL signal was spatially filtered by a 50 μm-pinhole and finally recorded by a single photon counter detector (Laser Components COUNT-10C). Additionally, a microwave field with a tuneable frequency was generated by a 100 μm diameter wire placed near the sample
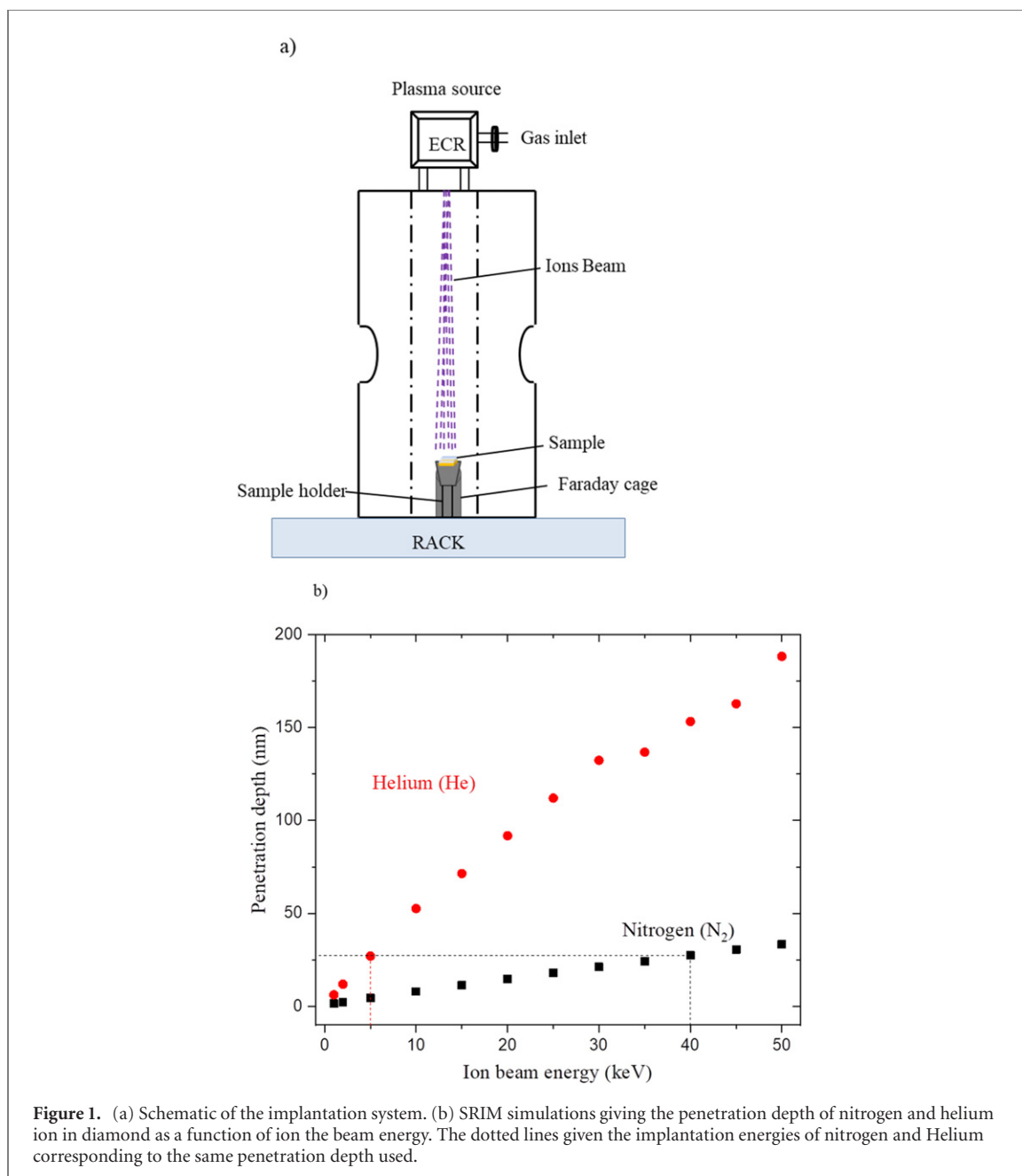
Figure 1. (a) Schematic of the implantation system. (b) SRIM simulations giving the penetration depth of nitrogen and helium ion in diamond as a function of ion the beam energy. The dotted lines given the implantation energies of nitrogen and Helium corresponding to the same penetration depth used.

Table 1. Surface treatments before implantation and irradiation conditions.

| Samples	Surface treatment before implantation	Irradiation conditions	Fluence (ions cm^{-2})	Surface treatment after implantation
1	As-grown/hydrogen termination	N_2^+ 10 s	2×10^{13}	Oxygen termination by ozone
2	As-grown/oxygen termination	N_2^+ 10 s	2×10^{13}	Oxygen termination by ozone
3	Polishing/acid cleaning/ hydrogen termination	N_2^+ 10 s/He$^+$ 10 s	$2 \times 10^{13}/4.1 \times 10^{12}$	Oxygen termination by ozone
4	Polishing/acid cleaning/ RIE-ICP etching/hydrogen termination	N_2^+ 10 s/He$^+$ 10 s	$2 \times 10^{13}/4.1 \times 10^{12}$	Oxygen termination by ozone
5	As-grown/hydrogen termination	N_2^+ 10 s/He$^+$ 0 s−10 s−20 s−30 s	$2 \times 10^{13}/0$−4.1×10^{12}− 8.2×10^{12}−1.2×10^{13}	Oxygen termination by O$_2$ plasma
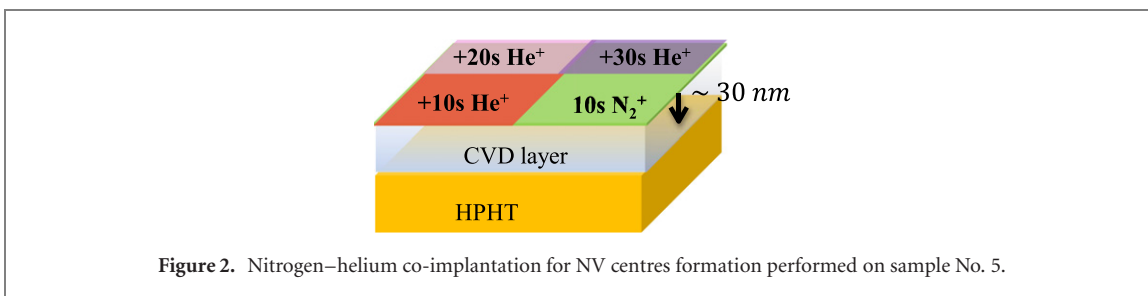
Figure 2. Nitrogen–helium co-implantation for NV centres formation performed on sample No. 5.
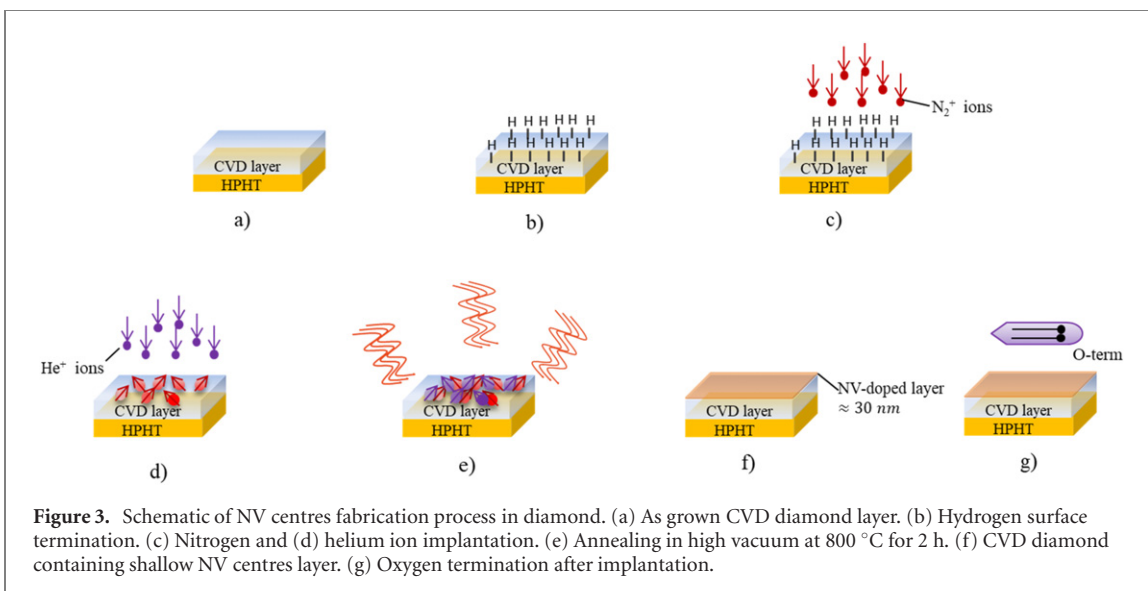

Figure 3. Schematic of NV centres fabrication process in diamond. (a) As grown CVD diamond layer. (b) Hydrogen surface termination. (c) Nitrogen and (d) helium ion implantation. (e) Annealing in high vacuum at 800 °C for 2 h. (f) CVD diamond containing shallow NV centres layer. (g) Oxygen termination after implantation.
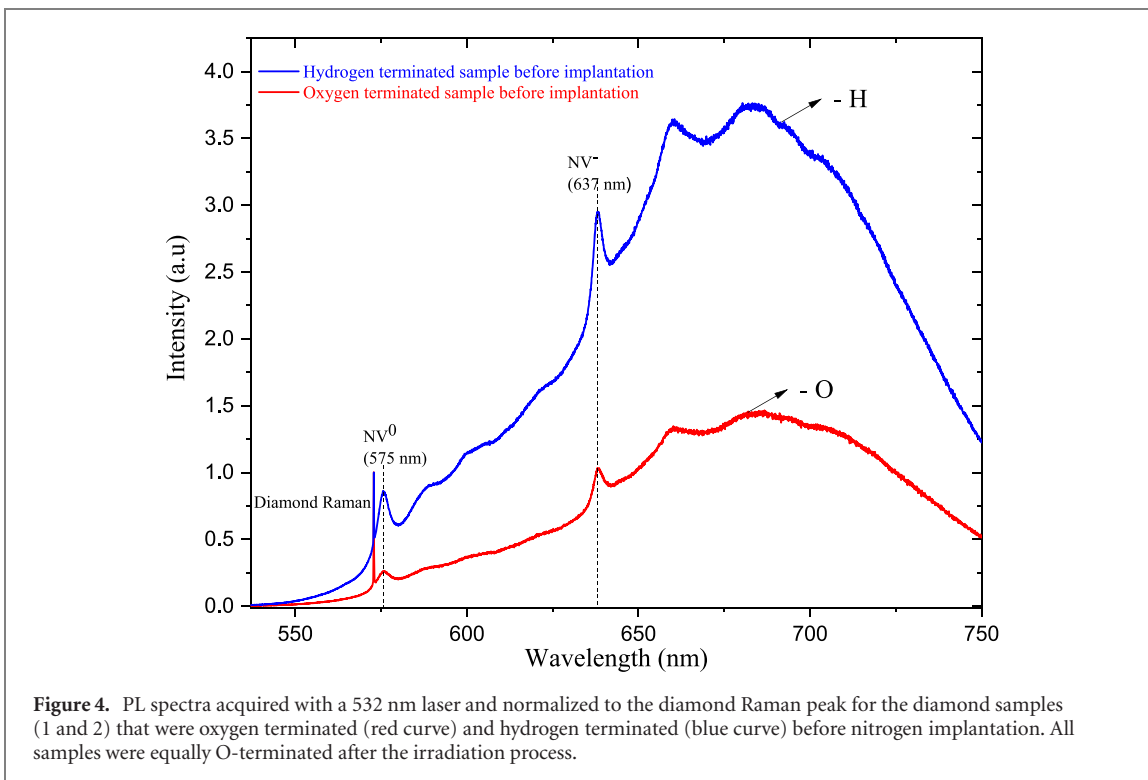

Figure 4. PL spectra acquired with a 532 nm laser and normalized to the diamond Raman peak for the diamond samples (1 and 2) that were oxygen terminated (red curve) and hydrogen terminated (blue curve) before nitrogen implantation. All samples were equally O-terminated after the irradiation process.
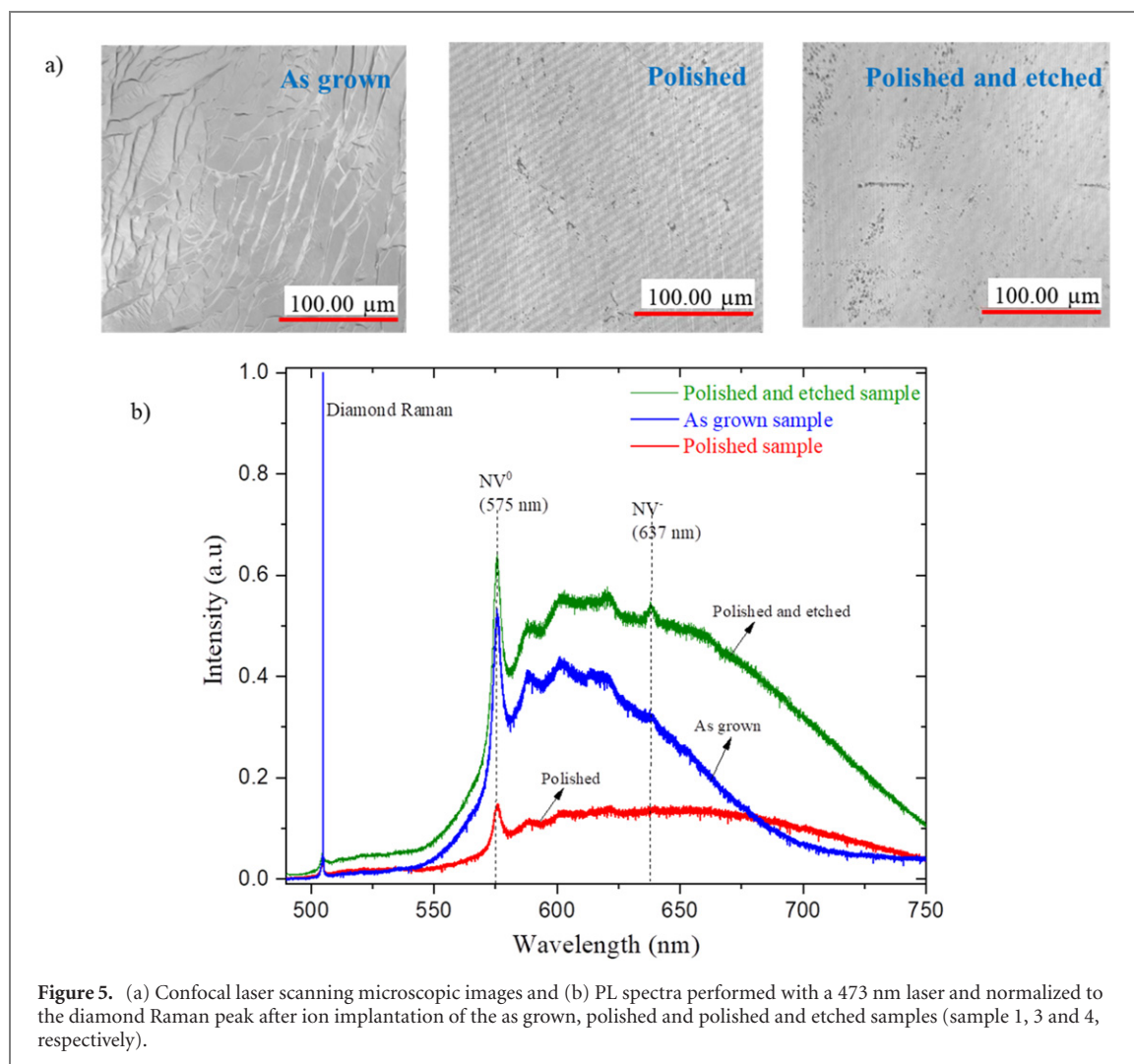
Figure 5. (a) Confocal laser scanning microscopic images and (b) PL spectra performed with a 473 nm laser and normalized to the diamond Raman peak after ion implantation of the as grown, polished and polished and etched samples (sample 1, 3 and 4, respectively).

surface and a permanent magnet has been used to lift the degeneracy of the $ms = \pm 1$ spin sublevels and completely separate lines pertaining to different NV orientations (by Zeeman effect). Thus, ODMR spectra were acquired by collecting the PL while sweeping the microwave frequencies: a PL intensity dip corresponds to a resonance between the microwave field frequency and the transition between $ms = 0$ and one of the $ms = \pm 1$ states (i.e., electron spin resonance ESR).
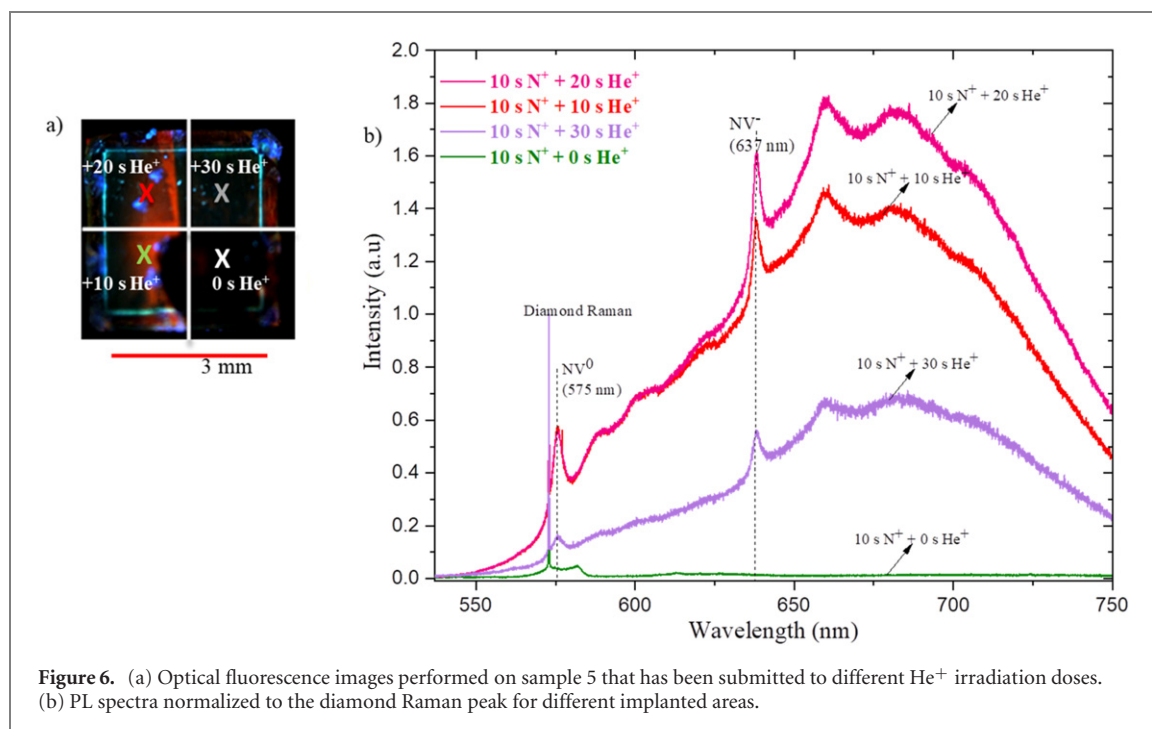
3. Results and discussion

3.1. Effect of surface termination on NV creation

PL analysis under optical laser excitation at 532 nm has been performed after nitrogen implantation and annealing on hydrogen and oxygen terminated CVD diamond samples (samples 1 and 2, respectively). We underline here again that after implantation all samples were equally oxygen terminated and therefore the effect of surface termination was only evaluated during the implantation process. Figure 4 shows the emission resulting from NV^0 and NV^- centres at 575 nm and 637 nm respectively. Both spectra have been normalized to the diamond Raman peak. Although NV centres have been successfully created whatever the surface termination before implantation, it can be noticed that for the hydrogen terminated sample the NV centres creation is more efficient. This is probably due to the fact that hydrogen-terminated diamond surfaces induces p-type surface transfer doping leading to a hole accumulation layer which could change the charge state of implantation defects and their recombination behaviour. In particular, the formation of thermally stable defects such as di-vacancy (V_2) or NVH could be strongly reduced as described by Fávaro de Oliveira *et al* [18].

3.2. Effect of polishing and RIE-ICP etching on NV creation

A critical issue for the formation of shallow NV centres in diamond is the surface roughness which has to be optimized for an implantation to a depth of a few nm. Surface roughness of the diamond films following CVD

Figure 6. (a) Optical fluorescence images performed on sample 5 that has been submitted to different He$^+$ irradiation doses. (b) PL spectra normalized to the diamond Raman peak for different implanted areas.

growth can indeed reach several tens of nm depending on the thickness. For therefore, it may be necessary to perform surface polishing. Figure 5 shows a comparison between the microscopic images and PL spectra acquired with a 473 nm laser excitation of the as-grown (sample 1), as-polished and polished followed by ICP etching samples (samples 3 and 4, respectively). The measurement by optical profilometry on an area of 100×100 μm^2 showed that the roughness has been reduced by the polishing from 0.8 μm for the as grown sample to 0.1 μm for the polished sample. It can be noticed that polishing has strongly reduced the NV centres creation efficiency. This is probably due to the fact that polishing induces sets of parallel polishing lines (figure 5(a)) produced by the abrasive particles moving across the surface even though it may appear smooth to the naked eye [19]. Moreover, it is well known that subsurface damage can be produced by the mechanical polishing [20]. In order to suppress these polishing effects, an additional surface treatment consisting in RIE-ICP etching has been performed. And as illustrated in figure 5(b), the PL spectrum of the polished and etched sample indicates higher creation efficiency for NV centres. This is believed to be due to the removal of subsurface damage induced by polishing and located in the first few micrometres at the surface that are etched away by the plasma.

3.3. Effect of helium co-implantation

PL imaging has been performed with the DiamondViewTM for sample 5 that has received different helium irradiation durations in different regions after nitrogen-helium co-implantation followed by thermal annealing. The result is presented in figure 6(a). Red luminescent regions are visible corresponding to the emission of NV centres created by the implantation process. We note here that the overall brightness is slightly reduced as compared to the previously implanted sample as reported in figure 4. This is likely due to the oxygen plasma termination performed at the end of the process that possibly etched away part of the surface NVs. Further optimization of this cleaning procedure should be performed. Nevertheless, the brightness difference between different regions already indicates a higher creation efficiency in the co-implanted areas with 10 and 20 s of treatment. Non-uniform NV creation is also visible within individual regions due to the ion distribution in the beam or to inaccurate positioning of the physical mask during irradiation.

To confirm this tendency, PL spectra performed at 532 nm laser excitation is given in figure 6(b). The presence of NV centres is clearly detected on the three parts of the diamond that have been implanted in a second step using He+ beam and it can be confirmed that an optimum is found for an implantation duration of 20 s. The region only implanted with nitrogen shows weak NV fluorescence. For too high an implantation dose (30 s), the NV fluorescence reduces again, probably due to graphitization of the diamond film or to the formation of defects that quench NV emission.

Figure 7(a) shows four typical ODMR spectra from the four different areas of the co-implanted sample. For the area that has not been implanted with helium, no electron spin resonance (ESR) contrast could be measured due to a too weak signal. For the other regions, the hyperfine interaction with 14N that has a $1/2$ spin
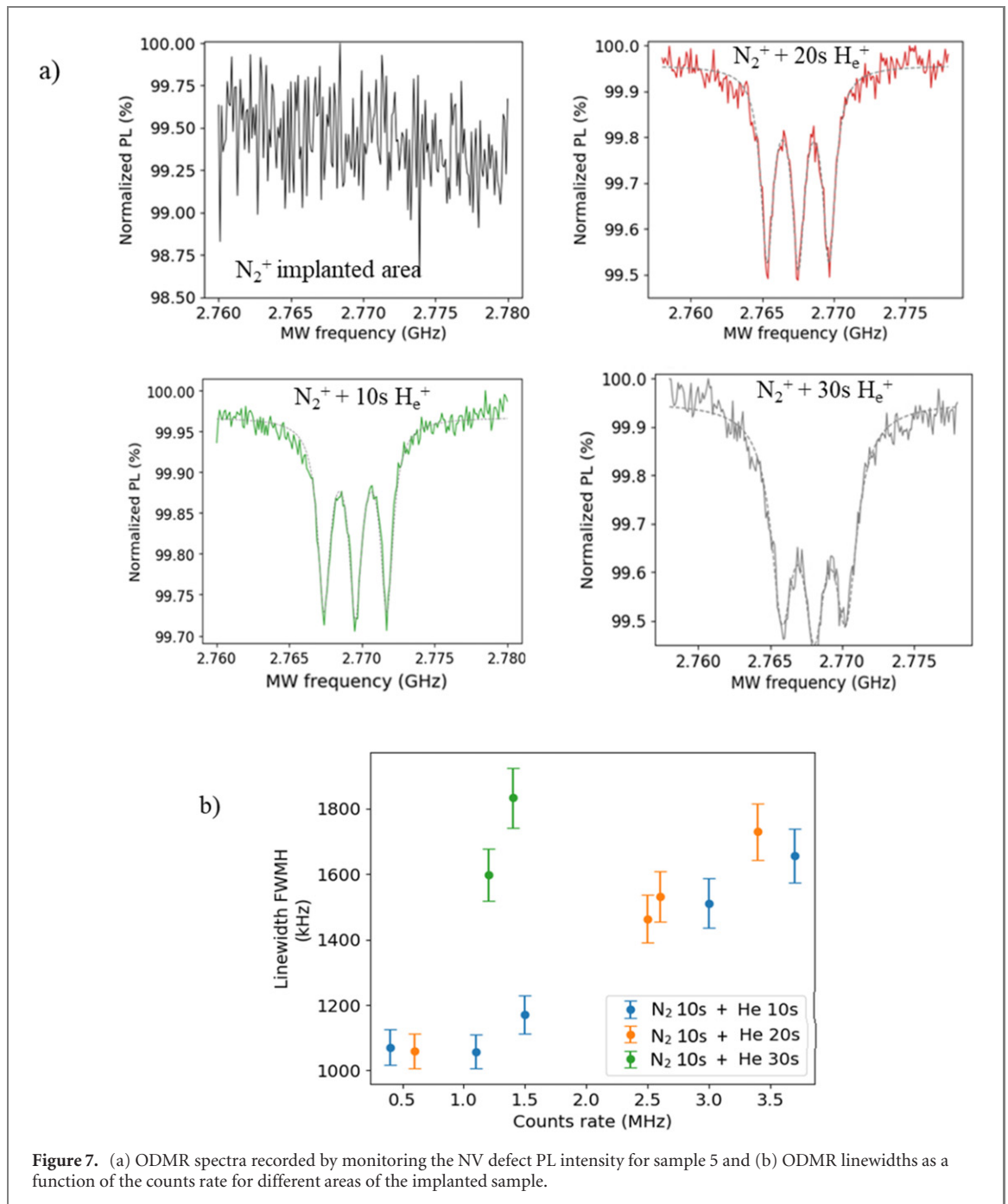
Figure 7. (a) ODMR spectra recorded by monitoring the NV defect PL intensity for sample 5 and (b) ODMR linewidths as a function of the counts rate for different areas of the implanted sample.

leads to the splitting of the ESR line into three components visible on the spectra. These measurements have been made repeatedly on several positions at each of the four different regions of the diamond surface. The ESR lines have been fitted with a Lorentzian and the extracted linewidth is plotted in figure 7(b). The extracted linewidth is equal or better than values already reported in the litterature [21–23]. An almost linear relationship between PL intensity and linewidth is observed for count rates larger than 1.1 MHz with a similar trend for the regions implanted with 10 and 20 s of He$^+$. Indeed, NV creation is not fully uniform over the implanted area and can vary by up to a factor of 7. For those areas with a moderate helium implantation time, NV density is likely to be the main limiting factor and the reason for the enlargement of the ESR lines. On the contrary, areas implanted for a longer time (30 s) always showed much weaker PL intensities but broad linewidth on the order of 1.7 MHz. In this case, it is believed that the presence of other defects or strain induced by the implantation is limiting ESR linewidth. Higher He$^+$ implantation doses are therefore not suitable to obtain bright intensity with narrow ESR linewidths. According to [24], the corresponding values of the coherence time ($T_2{}^*$) are calculated using the approximation

$$\mathbf{\Gamma} = 1/\left(\pi T_2^*\right)$$

Table 2. Full width at half maximum (FWHM) and coherence time (T_2^*) for the different implanted areas of sample 5.

Implanted area	FWHM (MHz)	T_2^* (ns)
N_2^+ only	Not enough signal	Not enough signal
N_2^+/10 s He^+ (three measurements)	1.05	301
	1.17	271
	1.51	210
N_2^+/20 s He^+ (three measurements)	1.06	300
	1.47	217
	1.53	208
N_2^+/30 s He^+ (two measurements)	1.6	199
	1.9	173

where Γ represents the full width at half maximum. These values are from 173 to 301 ns as given in table 2 and. In the regions implanted with 10 and 20 s of He, we have almost the same T_2^* values. While in the one implanted at 30 s of He we have smaller T_2^* values confirming the previously observed tendency.

4. Conclusion

Achieving shallow NVs with high concentrations and good spin properties in diamond is a real challenge, but it is a pre-requisite to the development of sensitive quantum sensors. Low energy ion implantation in high-quality CVD diamond films provides a way to achieve such near-surface NV ensembles but the optimization of this process is crucial. In this work we investigated different surface treatments prior to ion implantation and employed co-implantation with N_2^+ and He^+ with carefully chosen energies to reach similar range in matter. He^+ ions are used to add vacancies, and to improve substitutional nitrogen to NV conversion. We successfully created bright NV centre ensembles at about 30 nm from the CVD diamond surface and observed that this process is more efficient when moderate He^+ ion doses are used (4–8×10^{12} ions cm^{-2}). ODMR linewidths measured in continuous mode of the order of 1.5 MHz were achieved. In addition, we found that the initial surface state of the diamond samples prior to implantation strongly influences the creation efficiency of NVs. Hydrogen-terminated diamonds as well as surfaces without polishing-induced surface damage lead to a better NV creation yield. This approach will guide efforts to the development of diamond NV sensors with better sensitivity.

Acknowledgments

Data availability statement

All data that support the findings of this study are included within the article (and any supplementary files).

ORCID iDs

Midrel Wilfried Ngandeu Ngambou ⬥ https://orcid.org/0000-0002-0261-9072
Ionut Balasa ⬥ https://orcid.org/0000-0002-0147-9776
Fabien Bénédic ⬥ https://orcid.org/0000-0003-3350-4021
Philippe Goldner ⬥ https://orcid.org/0000-0001-8517-0911
Jocelyn Achard ⬥ https://orcid.org/0000-0001-7000-7230

References

[1] Gruber A, Dräbenstedt A, Tietz C, Fleury L, Wrachtrup J and von Borczyskowski C 1997 Scanning confocal optical microscopy and magnetic resonance on single defect centers *Science* **276** 2012–4
[2] Bar-Gill N, Pham L M, Jarmola A, Budker D and Walsworth R L 2013 *Nat. Commun.* **4** 1743
[3] Gaebel T *et al* 2006 *Nat. Phys.* **2** 408–13
[4] Li L *et al* 2015 *Nat. Commun.* **6** 6173
[5] Achard J, Jacques V and Tallaire A 2020 *J. Phys. D: Appl. Phys.* **53** 313001
[6] Suter D and Jelezko F 2017 *Prog. Nucl. Magn. Reson. Spectrosc.* **98–99** 50–62
[7] Jaffe T *et al* 2020 *Nano Lett.* **20** 3192–8
[8] Zhou T X, Stöhr R J and Yacoby A 2017 *Appl. Phys. Lett.* **111** 163106
[9] Fávaro de Oliveira F, Momenzadeh S Ali, Antonov D, Scharpf J, Osterkamp C, Naydenov B, Jelezko F, Denisenko A and Wrachtrup J 2016 *Nano Lett.* **16** 2228–33
[10] Meijer J, Burchard B, Domhan M, Wittmann C, Gaebel T, Popa I, Jelezko F and Wrachtrup J 2005 *Appl. Phys. Lett.* **87** 261909
[11] Morhange J F, Beserman R and Bourgoin J C 1975 *Japan. J. Appl. Phys.* **14** 544–8
[12] Naydenov B *et al* 2010 *Appl. Phys. Lett.* **96** 163108
[13] Khmelnitsky R A, Dravin V A, Tal A A, Zavedeev E V, Khomich A A, Khomich A V, Alekseev A A and Terentiev S A 2015 *J. Mater. Res.* **30** 1583–92
[14] Uzan-Saguy C, Cytermann C, Brener R, Ritcher M, Shaanan M and Kalish R 1995 *Appl. Phys. Lett.* **67** 1194–6
[15] Valentin A, De Feudis M, Brinza O, Tardieu A, William L, Tallaire A and Achard J 2018 *Phys. Status Solidi a* **215** 1800264
[16] Achard J, Silva F, Tallaire A, Bonnin X, Lombardi G, Hassouni K and Gicquel A 2007 *J. Phys. D: Appl. Phys.* **40** 6175–88
[17] Ziegler J F, Ziegler M D and Biersack J P 2010 *Nucl. Instrum. Methods Phys. Res.* B **268** 1818–23
[18] Fávaro de Oliveira F 2017 *Nat. Commun.* **8** 15409
[19] Chen Y and Zhang L 2013 *Polishing of Diamond Materials* (*Engineering Materials and Processes*) (London: Springer)
[20] Achard J, Tallaire A, Mille V, Naamoun M, Brinza O, Boussadi A, William L and Gicquel A 2014 *Phys. Status Solidi a* **211** 2264–7
[21] Osterkamp C, Balasubramanian P, Wolff G, Teraji T, Nesladek M and Jelezko F 2020 *Adv. Quantum Tech.* **3** 2000074
[22] Tetienne J *et al* 2018 *Phys. Rev.* B **97** 085402
[23] van Dam S B *et al* 2019 *Phys. Rev.* B **99** 161203
[24] Barry J F, Schloss J M, Bauch E, Turner M J, Hart C A, Pham L M and Walsworth R L 2020 *Rev. Mod. Phys.* **92** 015004